Dynamic Characterization of KUKA Light-Weight Robot Manipulators

Technical Report GT-RIM-CR-2012-001

Jacob Huckaby and Henrik I. Christensen

Center for Robotics & Intelligent Machines
Georgia Institute of Technology
801 Atlantic Drive NW
Atlanta, GA 30332, USA
huckaby@gatech.edu, hic@cc.gatech.edu

1 Introduction

High precision tasks are an important part of the manufacturing industry. For example, safety constraints require that some manufacturing must be done to a very high degree of accuracy. Robotics and automation are well suited for such tasks, as there is high repeatability on specialized repetitive tasks. Robotics has a long history in manufacturing in the form of industrial automation. Yet these robotic systems tend to be very large, restricting their use to tasks in open spaces that are easily accessible to the robot.

In the last few years there have been a number of advances in the area of small, light weight robots. One such robot is the KUKA Light-Weight Robot (LBR) [1]. With the availability of smaller robot manipulators, the question arises of whether it would be feasible to use them in tasks that would otherwise be unsuitable for the standard large industrial robots. Possible tasks would be those in tight or constrained spaces, such as in sub-structure drilling. For this to be possible, the light weight robot would need to be stiff enough to be able to meet safety constraints.

To that end, this study is to determine whether the dynamic characteristics, specifically stiffness, of small light weight robots would make it possible for them to be used in manufacturing. Two light weight robots are considered in this study, the LBR and the KUKA KR5 sixx.

2 Technical Background

Modal analysis is a method for finding the dynamic characterization of a system. An underlying assumption in modal analysis is that for linear systems, the vibration response of the system can be decomposed into a set of vibrational modes. A single system mode is characterized by a number of parameters, such as modal stiffness, modal damping, modal mass, and natural frequency.

Experimental modal analysis involves the test and measurement of the response of a physical system, and the determination of the dynamic system characteristics (i.e., modal parameters.) Experimental modal analysis is composed of three major parts: test preparation, measurement, and analysis. In test preparation it is important to select appropriate inputs and sensors, check sensor placement for good readings, and do initial data processing to check for linearity and reciprocity. During measurement, a force input and vibration response are measured for the system using a data capture device (for example, a signal analyzer.) Force input can be provided with an impulse hammer or a shaker, while vibration response is usually measured with accelerometers. Analysis is concerned with processing measurement data, and using the resulting frequency response function to determine dynamic characteristics.

A frequency response function (FRF) is complex function that reflects the relationship between a given input and the system vibratory response. It is analysis of the FRF obtained in measurement that determines modal parameters. In general, data measured with an accelerometer will yield what is known as an accelerance FRF. Using the notation found in [2], the accelerance FRF is defined as

$$A(\omega) = \frac{\ddot{X}(\omega)}{F(\omega)}$$

where $\ddot{X}(\omega)$ is the acceleration response and $F(\omega)$ is the force input. A more useful form of the FRF is the receptance (or compliance) FRF $\alpha(\omega)$, where

$$\alpha(\omega) = \frac{X(\omega)}{F(\omega)}.$$

This receptance FRF is easily obtained from $A(\omega)$ with the relationship

$$|A(\omega)| = \omega^2 |\alpha(\omega)|.$$

Once an appropriate FRF has been found, there are a number of methods that calculate the modal parameters for each system mode.

Coherence is another useful tool in the analysis of frequency response. The coherence represents a measure of the linearity and causality of the input to the output signal. This is important to the analysis because one of the fundamental assumptions in modal analysis is system linearity. A common method for determining coherence is the magnitude-squared method

$$C_{xy}(\omega) = \frac{|P_{xy}(\omega)|^2}{P_{xx}(\omega) P_{yy}(\omega)},$$

where $C_{xy}(f)$ is the magnitude squared coherence, $P_{xy}(f)$ is the cross-spectrum power density, and $P_{xx}(f)$ and $P_{yy}(f)$ are respectively the input and output spectrum power densities. When the system output is a direct result of the input the coherence measure is 1, and coherence is 0 when there is no correlation between input and output signals. Poor coherence can have many causes, among them system nonlinearities, bad signal to noise ratio, and human error.

3 Hardware Description

The two robots used in this project are the KUKA KR5 sixx, and the KUKA Light-Weight Robot.

3.1 KUKA KR5 sixx

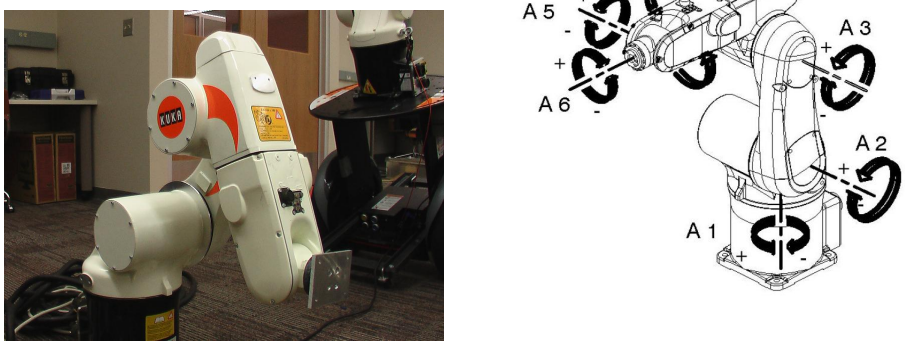

Fig. 1: KUKA KR5-sixx

The KUKA KR5 sixx is a 6 degree-of-freedom robot manipulator that is targeted toward light manufacturing and industrial tasks. It has a payload of 5 kilograms (11 pounds) and a maximum reach / workspace of 650 mm (2.13 feet.)

3.2 KUKA LBR

The KUKA Light-weight Robot, or LBR, is the second robot manipulator utilized in this project. The LBR is a 7 degree-of-freedom robot developed by DLR (German Aerospace Center) and sold by KUKA. It is currently one of the more advanced robot arms available, and uses harmonic drive gears and multiple sensors in each joint of the arm. The LBR is capable of joint, torque, and impedance control (though these features are not used in this experiment.) It has a payload of 14 kg (30 pounds) and a maximum reach / workspace of 936 mm (3.07 feet.) The main control loop running on the robot controller samples commands at a rate of 1 kHz.

4 Experimental Protocol

The typical setup for performing modal analysis impulse testing involves using an impact hammer to excite the structure being tested, an accelerometer to

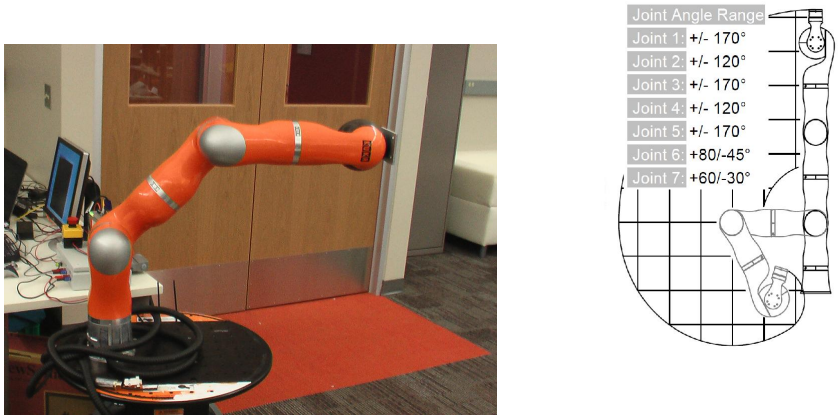

Fig. 2: KUKA LBR

measure the dynamic response, and a data gathering device to record both the input to and output of the system.

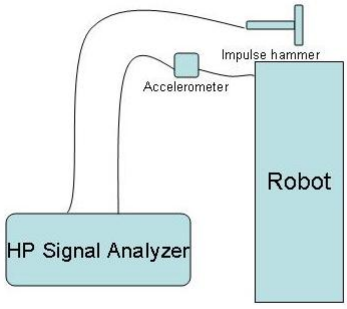

Fig. 3: Hardware Setup

The data gathering device for this experiment was a Hewlett-Packard HP3562A Dynamic Signal Analyzer. The signal analyzer received signals from both the accelerometer and the impact hammer, and the data was then transferred to a separate PC via a LabVIEW GPIB interface.

A single-axis accelerometer was rigidly attached to the end effector of the manipulator, aligned with each major axis. An impulse from the hammer was

given along the accelerometer measurement axis, and data was recorded from both sensors. This test was repeated several times for each major axis.

The force stimulus was provided by a PCB Piezotronics 086C03 impulse hammer. The underlying goal was to excite the broadest range of frequencies to get a clear picture of the dynamic performance of the manipulator. The range of frequencies excited can be controlled by the type of tip used to make contact with the robot (for example a soft rubber tip or a steel tip.) After a number of tests, a hard rubber tip was selected for both robots.

5 Results & Analysis

5.1 KR5 sixx

Figures 4 through 7 show the averaged coherence and compliance FRF response plots along the major axes for the KR5 sixx. Resonant frequencies common across major axes can be seen at 13 Hz and 45Hz with a compliant measure of 10^{-2} mm/N.

KR5 sixx	
Frequency (Hz)	*Compliance(mm/N)*
13	10^{-2}
45	10^{-1} - 10^{-2}

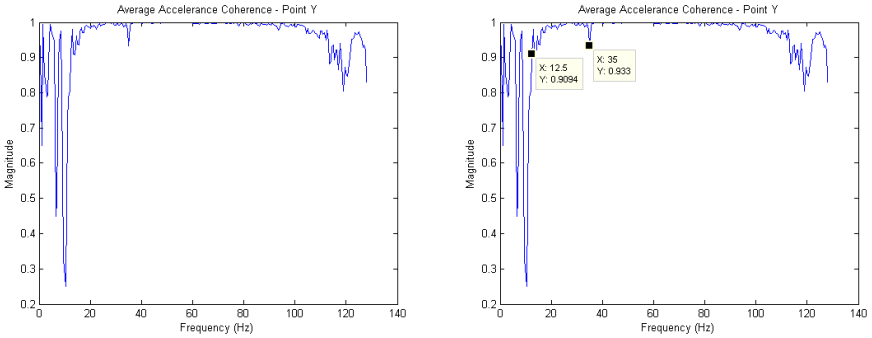

(a) Coherence 1 (b) Coherence 2

Fig. 4: KR5 sixx coherence graph along global Y axis

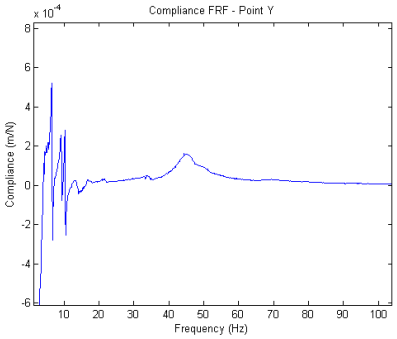

(a) Compliance 1

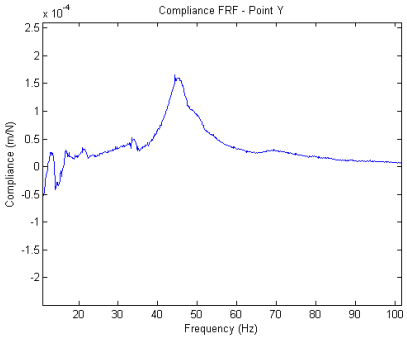

(b) Compliance 2

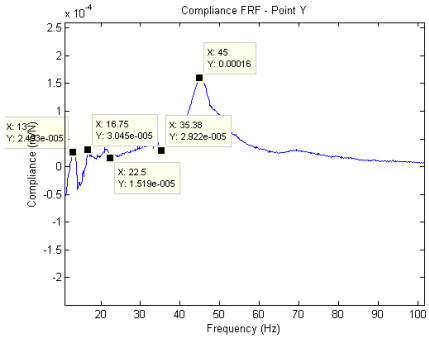

(c) Compliance 3

Fig. 5: KR5 sixx averaged compliance FRF along global Y axis

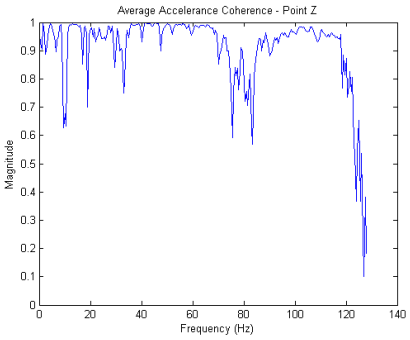

(a) Coherence 1

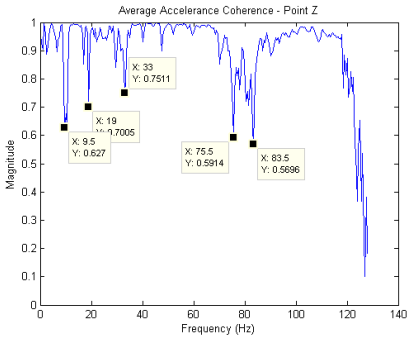

(b) Coherence 2

Fig. 6: KR5 sixx coherence graph along global Z axis

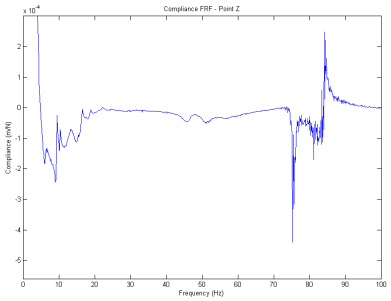

(a) Compliance 1

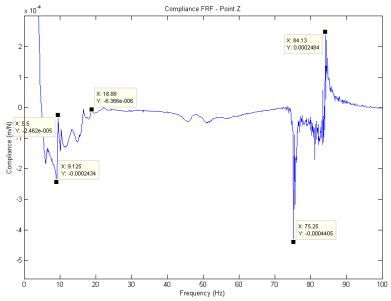

(b) Compliance 2

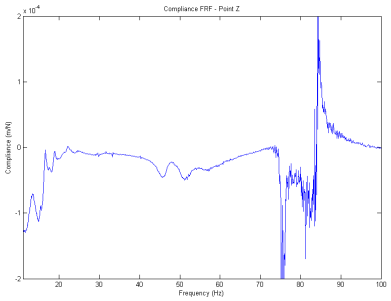

(c) Compliance 3

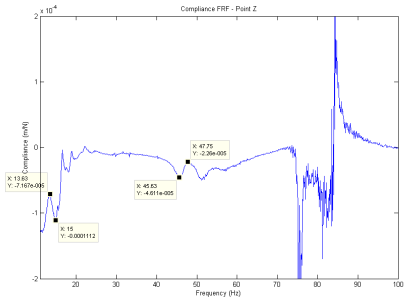

(d) Compliance 4

Fig. 7: KR5 sixx averaged compliance FRF along global Z axis

5.2 LBR

Figures 8 through 23 show the response plots for three different configurations of the LBR. Based on the coherence graphs, analysis is done between 12Hz and 115Hz. Given this analysis, across all of the tested poses we could expect to see some form of resonance at 20Hz and at 100Hz within the same range of dynamic compliance.

Pose 1	
Frequency (Hz)	*Compliance(mm/N)*
20	10^{-2}
44	10^{-1} - 10^{-2}
100	10^{-4}

Pose 2	
Frequency (Hz)	*Compliance(mm/N)*
13	10^{-2}
45	10^{-1} - 10^{-2}

Pose 3	
Frequency (Hz)	*Compliance(mm/N)*
13	10^{-2}
45	10^{-1} - 10^{-2}

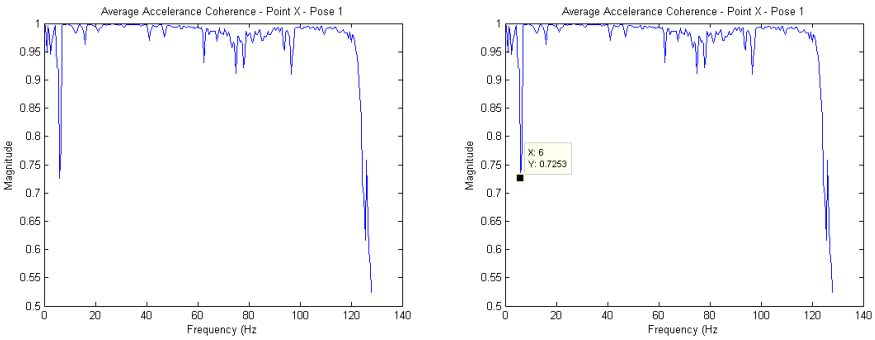

(a) Coherence 1 (b) Coherence 2

Fig. 8: LBR coherence graph along global X axis - Pose 1

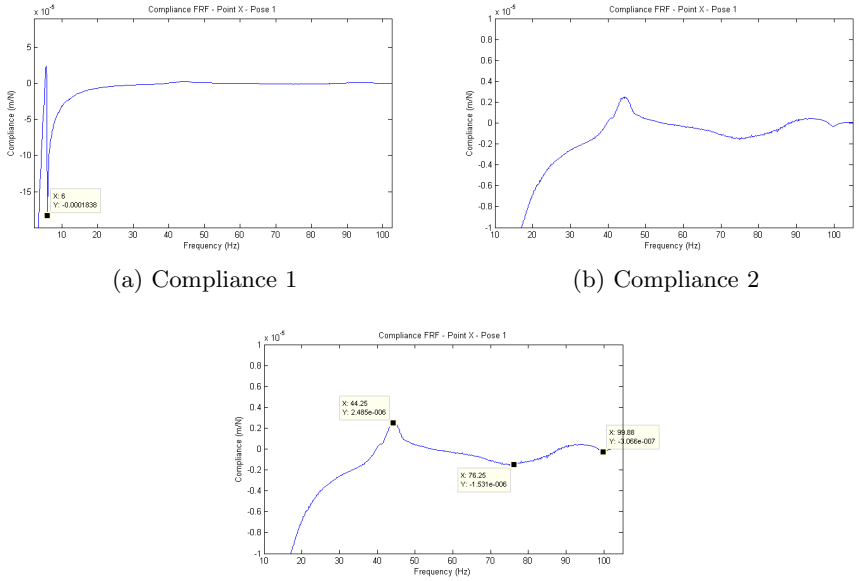

(a) Compliance 1 (b) Compliance 2

(c) Compliance 3

Fig. 9: LBR averaged compliance FRF along global X axis - Pose 1

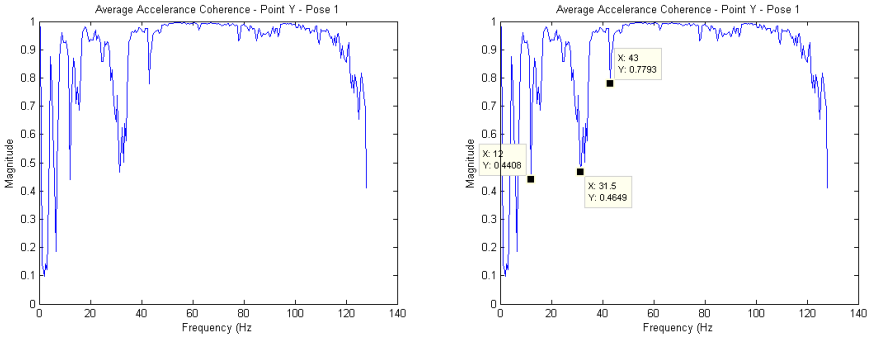

(a) Coherence 1 (b) Coherence 2

Fig. 10: LBR coherence graph along global Y axis - Pose 1

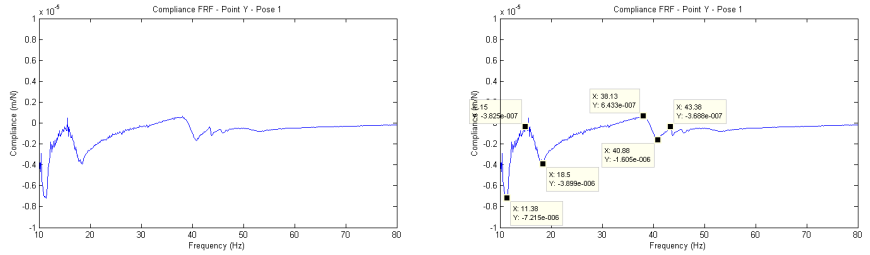

(a) Compliance 1 (b) Compliance 2

Fig. 11: LBR averaged compliance FRF along global Y axis - Pose 1

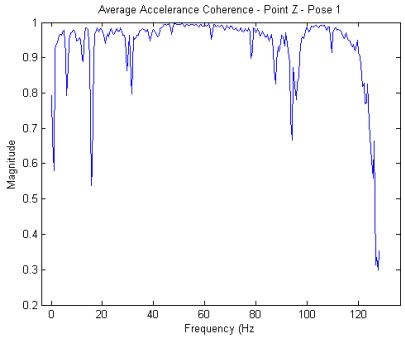

(a) Coherence 1

Fig. 12: LBR coherence graph along global Z axis - Pose 1

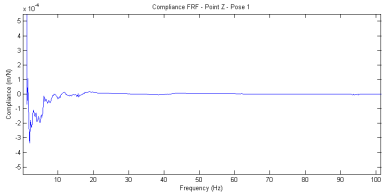

(a) Compliance 1

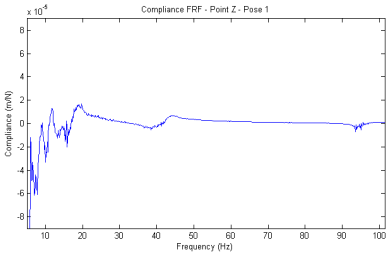

(b) Compliance 2

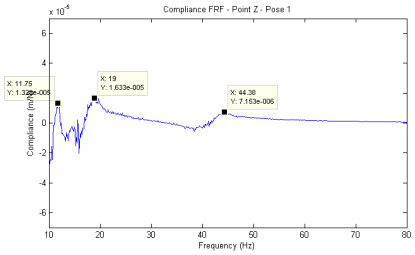

(c) Compliance 3

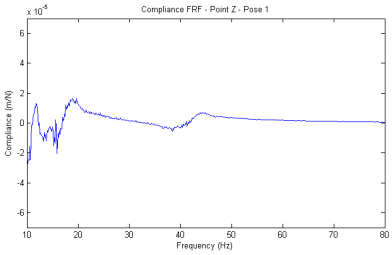

(d) Compliance 4

Fig. 13: LBR averaged compliance FRF along global Z axis - Pose 1

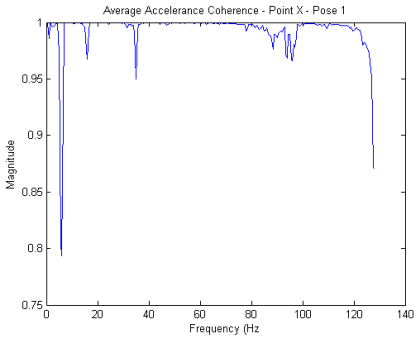

(a) Coherence 1

Fig. 14: LBR coherence graph along global X axis - Pose 2

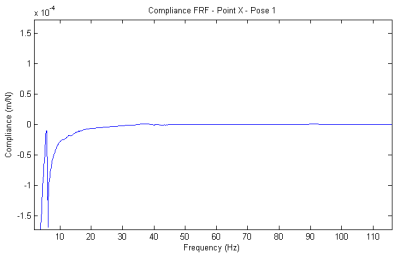

(a) Compliance 1

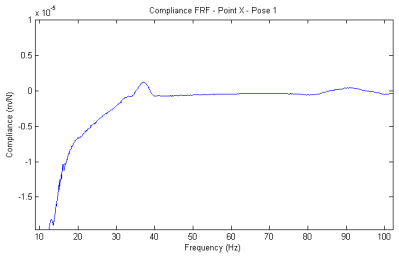

(b) Compliance 2

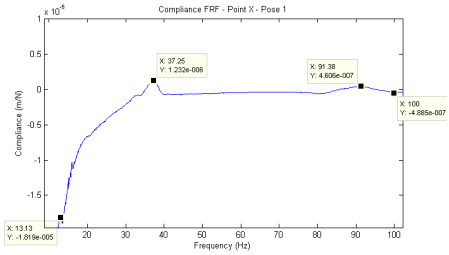

(c) Compliance 3

Fig. 15: LBR averaged compliance FRF along global X axis - Pose 2

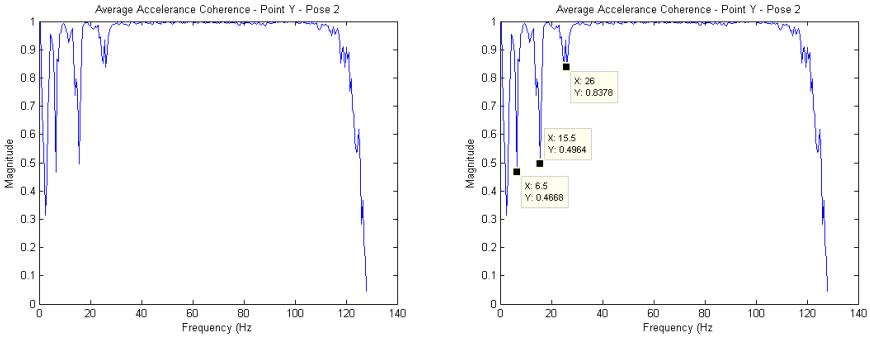

(a) Coherence 1 (b) Coherence 2

Fig. 16: LBR coherence graph along global Y axis - Pose 2

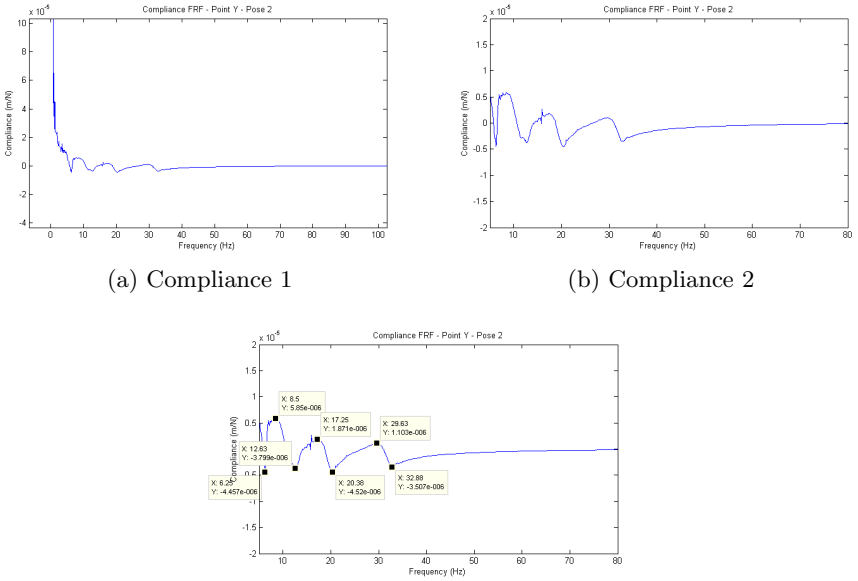

(a) Compliance 1 (b) Compliance 2

(c) Compliance 3

Fig. 17: LBR averaged compliance FRF along global Y axis - Pose 2

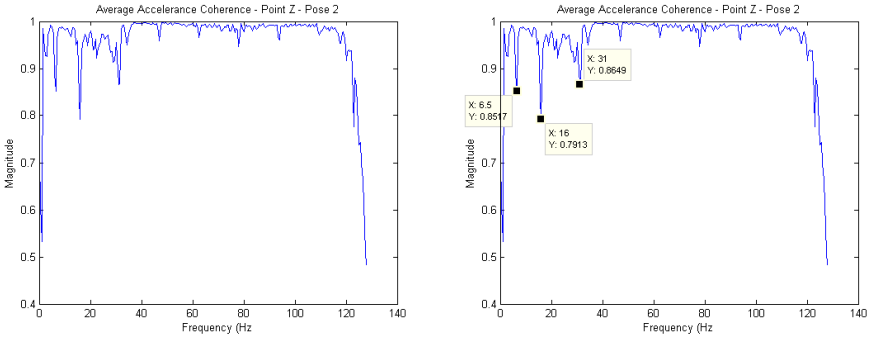

(a) Coherence 1 (b) Coherence 2

Fig. 18: LBR coherence graph along global Z axis - Pose 2

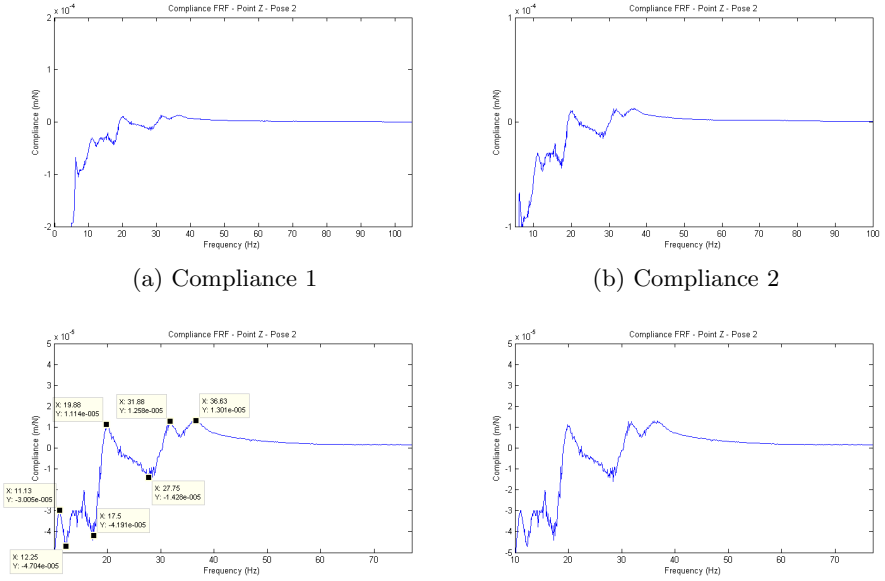

(a) Compliance 1 (b) Compliance 2

(c) Compliance 3 (d) Compliance 4

Fig. 19: LBR averaged compliance FRF along global Z axis - Pose 2

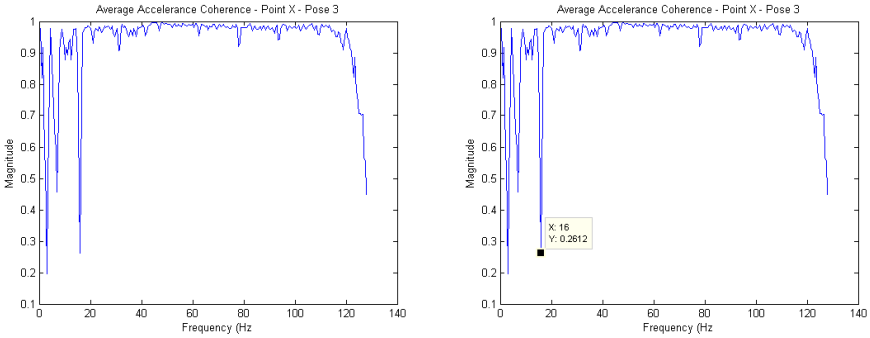

(a) Coherence 1 (b) Coherence 2

Fig. 20: LBR coherence graph along global X axis - Pose 3

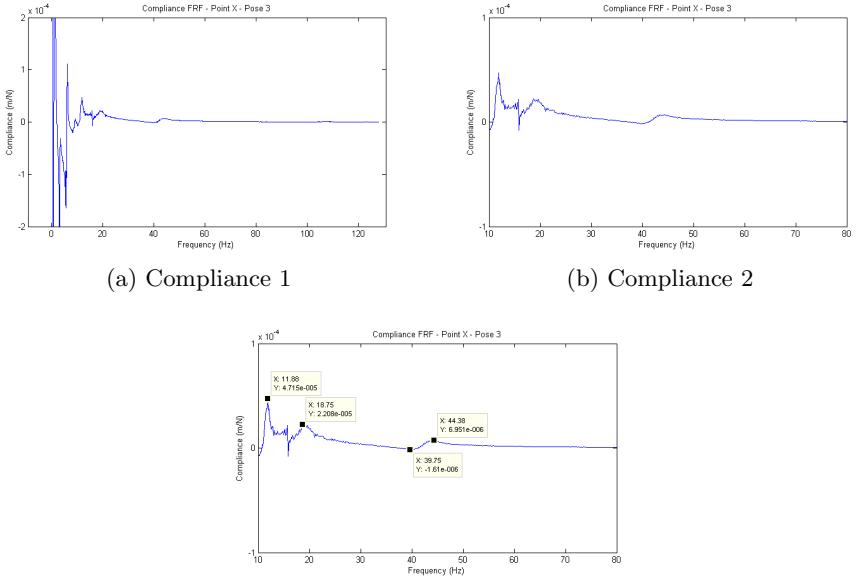

(a) Compliance 1 (b) Compliance 2

(c) Compliance 3

Fig. 21: LBR averaged compliance FRF along global X axis - Pose 3

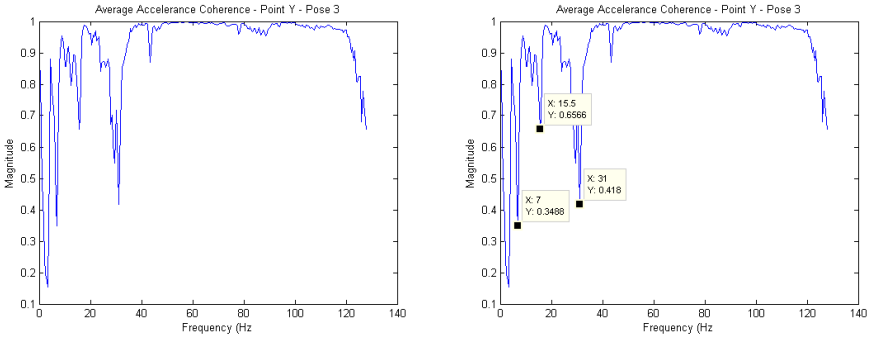

(a) Coherence 1 (b) Coherence 2

Fig. 22: LBR coherence graph along global Y axis - Pose 3

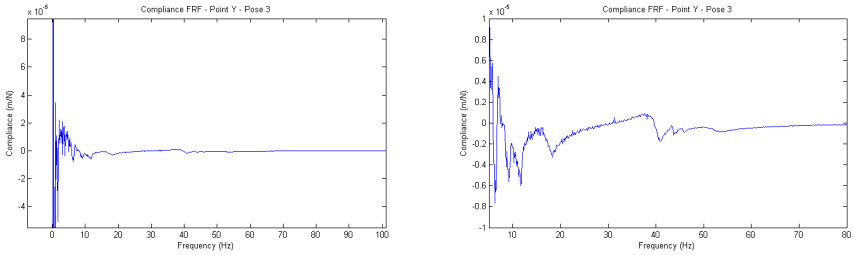

(a) Compliance 1 (b) Compliance 2

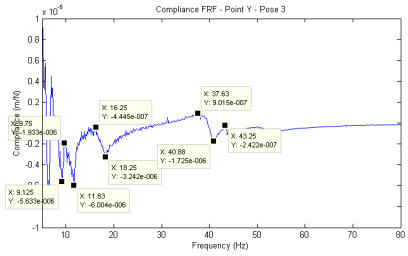

(c) Compliance 3

Fig. 23: LBR averaged compliance FRF along global Y axis - Pose 3

5.3 Analysis

During analysis, a number of the tests were discarded due to poor coherence. Coherence graphs with a greater range of frequencies below 80 percent were deemed to be too unreliable. There are a number of reasons that could account for this. One of the difficulties with impulse testing in modal analysis is the inability to perfectly recreate input into the system. While most of the energy put in may lie along the measuring axis, some energy will unavoidably be dispersed along minor axes. While this can be limited to a degree by careful execution of the testing, it is difficult to quantify the amount of energy lost in each individual test.

Another possible cause of poor coherence are nonlinearities in the mechanical system. For example, the LBR uses joint torque sensors in each joint to do active vibration damping, which uses a full state feedback controller to actively suppress vibration along the link. This type of internal adjustment could easily affect coherence linearity. And while some of these issues may have corrupted a portion of the gathered data, there was enough usable data to gain insight into the behavior of both of the robots.

The graphs presented in the previous section indicated the resonant frequencies of each manipulator, as well as the relative compliances at those resonant frequencies. Resonant frequencies were measured at the dominant peaks of the compliance FRF, and compliance was identified at the resonant peaks. Based on those measures, the plots show that the LBR is on average as stiff as or stiffer than the KR5 sixx across the 0-100Hz range. Comparing the 12/13Hz and 44/45Hz resonant frequencies found in both the KR5 sixx and two poses of the LBR, the LBR is within the same compliant range of the KR5 sixx, or an order of magnitude stiffer.

6 Conclusion

In this report, an analysis was made of the dynamic characteristics of two KUKA robot manipulators, specifically the dynamic compliance, and a comparison was made between each robot's dynamic performance. In the tests performed, the LBR measured as stiff as or stiffer than the KR5 sixx across the 0-100Hz frequency range.

References

[1] Hirzinger, G.; Sporer, N.; Albu-Schffer, A.; Hhnle, M.; Krenn, R.; Pascucci, A.; Schedl, M. (2002): DLR's torque-controlled light weight robot III - are we reaching the technological limits now? In: Proceedings ICRA 2002, S. 1710 - 1716, IEEE International Conference on Robotics and Automation ICRA, Washington D.C., USA, May 2002

[2] He, J., Fu, Z. (2001). *Modal analysis.* Oxford: Butterworth-Heinemann.